

Converting entanglement into ensemble basis-free coherence

A. Kodukhov*

Terra Quantum AG, Kornhausstrasse 25, St. Gallen, Switzerland, 9000

* *ak@terraquantum.swiss*

The resource theory of coherence addresses the extent to which quantum properties are present in a given quantum system. While coherence has been extensively studied for individual quantum states, measures of coherence for ensembles of quantum states remain an area of active research. The entanglement-based approach to ensemble coherence — where a partial measurement of an entangled state generates an ensemble — relates the ensemble coherence to both the initial entanglement and the measurement’s uncertainty. This paper presents two methods for generating ensemble coherence from a fixed amount of entanglement. The first method involves applying a von Neumann measurement to one part of a non-maximally entangled bipartite state, resulting in a pair of non-orthogonal states whose coherence can equal the initial entanglement. The second method considers a class of symmetric observables capable of generating ensembles used in quantum key distribution (QKD) protocols such as B92, BB84, and three-state QKD. As a result, this work contributes to understanding how much ensemble coherence can be obtained from a given amount of entanglement.

I. Introduction

Since the establishment of quantum mechanics, there has been an ongoing debate about the boundary between quantum and classical phenomena. Bohr and Einstein famously disagreed over the existence and implications of the uncertainty principle as a genuinely quantum feature. This foundational debate ultimately favored Bohr’s interpretation [1]. In the second half of the 20th century, attention shifted toward understanding whether it is possible to extract partial information about two non-commuting observables, particularly in the context of the double-slit interference experiment [2, 3].

Today, we are witnessing the rapid emergence of quantum technologies, promising breakthroughs in computation and secure communication. These developments require a formal and quantitative understanding of the quantum properties of the states employed in quantum devices. In the modern framework of quantum information theory, this role is fulfilled by the resource theory of coherence. The resource theory of coherence has been thoroughly developed for individual density matrices [4–7], with detailed analyses of its dynamics under various decoherence processes relevant to quantum algorithms, metrology and other areas [8, 9]. Coherence is also studied in the conditions of relativistic motion that appeared to be an additional source of decoherence [10]. Importantly, resource theories also provide a structured framework for converting different quantum quantities — for example, determining how much coherence can be generated from a given amount of entanglement, and vice versa [11–15].

In another important direction of quantum technologies, quantum cryptography, ensembles of quantum states are used instead of individual density matrices. For instance, characterizing ensemble properties is essential for estimating the amount of information an adversary could extract about a shared bit string. Conversely, legitimate users need to assess how much secret key can be obtained from a given ensemble. This motivates the ex-

ension of the resource theory of coherence to ensembles of quantum states.

The active discussion of how much quantumness is contained in an ensemble of states was initiated by C.A.Fuchs in the context of two non-orthogonal states [16]. As a measure of ensemble quantumness, he proposed, for example, the gap between the Holevo quantity and the accessible information, as well as the achievable fidelity in cloning an unknown state drawn from the ensemble. Later, C.A.Fuchs and M.Sasaki introduced a related quantumness measure based on the worst-case difficulty of transmitting ensemble states through a classical communication channel [17]. Subsequent studies have proposed a variety of alternative measures for ensemble quantumness. In Refs. [18–20], the measure is based on the Gram matrix of the ensemble. This matrix, which can be interpreted as a density matrix, encodes the pairwise overlaps between all states in the ensemble. Quantumness is then quantified using the relative entropy of coherence [4, 21, 22] or the l_1 -norm [4, 23] of the Gram matrix. Another approach defines ensemble quantumness via the Rényi entropy of the Gram matrix [24]. In Ref. [6], a different measure is introduced based on unitary similarity-invariant norms of the commutators between the ensemble’s density matrices. A final, but equally important, approach defines ensemble quantumness as the average (over the ensemble) of the relative entropy of coherence, minimized over all possible bases. This quantity was first introduced in Refs. [25–27] and was independently developed further in Refs. [28, 29]. Importantly, this measure is basis-free and effectively quantifies the extent to which the states of an ensemble cannot be simultaneously diagonalized.

Ref. [29] analytically demonstrated that an ensemble can be generated by performing a local measurement on one part of an entangled bipartite state [30]. When an observer applies an arbitrary POVM to their subsystem, an ensemble of post-measurement states is created in the other subsystem. The resulting ensemble coherence (or quantumness) depends on both the entangle-

ment consumption and the uncertainty of the applied measurement, where the latter corresponds to the unpredictability of measurement outcomes. Moreover, the entanglement-based approach to coherence also describes the quantum interference, particularly in the frameworks introduced by Englert [3] and by Wootters & Zurek [2].

This study develops several methods for generating ensemble coherence from a given amount of initial entanglement. The first method involves producing a pair of non-orthogonal states via a von Neumann measurement on one part of a non-maximally entangled bipartite state. For relatively low initial entanglement, the resulting ensemble's basis-free coherence equals the entanglement, coinciding with the upper bound derived in Ref. [29]. The second method explores a class of symmetric observables that, in principle, can exhibit arbitrarily high measurement uncertainty. However, an unlimited increase in uncertainty does not yield unbounded coherence; instead, the ensemble coherence saturates at a finite level. Within this class of symmetric observables, one can generate ensembles corresponding to various QKD protocols, including B92 [31], BB84 [32], and three-state QKD [33, 34]. As a result, this study contributes to establishing the dependence of constructively achievable coherence on the initial entanglement.

II. Entanglement-based approach to coherence

An ensemble of quantum states can be obtained by a local measurement of one subsystem of a bipartite entangled state. Let Alice (A) — the holder of one of two finite-dimension subsystems — apply a local positive operator-valued measure (POVM) to their part of the entangled state. Then, the holder of the second subsystem, Bob (B), observes an ensemble of quantum states. The observed density matrix on Bob's side depends on Alice's obtained measurement result. The process of ensemble generation was initially suggested in Refs. [30, 35] and fully formalized in Ref. [29].

The entangled state can be written in the Schmidt decomposition

$$|\Psi\rangle_{AB} = \sum_{n=1}^d \sqrt{\lambda_n} |n\rangle_A |n\rangle_B, \quad (1)$$

where d is the dimension of each subsystem, $\sqrt{\lambda_n}$ are Schmidt coefficients and $\{|n\rangle_A |n\rangle_B\}_n$ is the Schmidt basis. In the Schmidt basis, the partial density matrices of each subsystem naturally has diagonal form

$$\sigma_{A(B)} = \sum_{n=1}^d \lambda_n |n\rangle\langle n|_{A(B)}. \quad (2)$$

A pure bipartite entangled state can be characterized by its entanglement measure. In the simplest case, the entanglement is defined as a the von Neumann entropy of

any of two subsystems [35–37]

$$E(|\Psi\rangle_{AB}) = S(\sigma_B) = - \sum_{n=1}^d \lambda_n \log_2 \lambda_n. \quad (3)$$

The latter equality arises when considering the diagonal form of the reduced density matrices. In this case, the entanglement corresponds to the classical Shannon entropy of the squared Schmidt coefficients. The shared state between Alice and Bob is maximally entangled when all Schmidt coefficients are equal. Conversely, the state is separable when only one Schmidt coefficient is non-zero.

Alice applies observable \mathcal{M}_A with the POVM elements $M_i^{(A)}$ ($i = 1, \dots, N$) to their part of the entangled state. Bob observes an ensemble \mathcal{E}_B of quantum states ρ_i with probabilities p_i

$$\mathcal{E}_B = \left\{ p_i = \text{tr} \left(\sigma_A M_i^{(A)} \right), \rho_i = \frac{1}{p_i} \sqrt{\sigma_B} M_i^{(B)} \sqrt{\sigma_B} \right\}_i, \quad (4)$$

where

$$M_i^{(B)} = \sum_{m,n} \langle m | M_i^{(A)} | n \rangle_A | n \rangle \langle m |_B. \quad (5)$$

The ensemble obeys the similar probability distribution as measurement results on Alice's side. Operators $M_i^{(B)}$ have the same matrix elements as POVM operators $M_i^{(A)}$, but act in Bob's subsystem.

Alice's POVM can be characterized by the quality of uncertainty with respect to the measured entangled state. Motivation for this quality is raised from the entropic uncertainty relations for a single observable [38–40]. Firstly, we define the entropy of measurement results, when a POVM \mathcal{M} is applied to an arbitrary density matrix

$$U(\mathcal{M}|\rho) = - \sum_{i=1}^N \text{tr}(M_i \rho) \log_2 \text{tr}(M_i \rho), \quad (6)$$

where M_i is a POVM element of the considered observable and ρ is a probe density matrix. The uncertainty of POVM with respect to the bipartite entangled state shows the unpredictability of measurement results, when a POVM is applied to one of the subsystems

$$U(\mathcal{M}|\Psi\rangle_{AB}) = \min_{\mathcal{E}_A} \sum_k p(k) U(\mathcal{M}|\rho_k), \quad (7)$$

$$\mathcal{E}_A = \{p(k), \rho_k\}_k : \sum_k p(k) \rho_k = \sigma_A.$$

The minimum is taken over all possible decompositions of Alice's reduced density matrix σ_A , and is achieved by decompositions consisting of pure states.

Before providing the coherence definition for an ensemble, we remind the framework for a single quantum state. To define coherence of a density matrix ρ , one usually utilizes the relative entropy of coherence [4, 8]

$$C_{\text{rel}}(\rho) = S(\rho|\rho^{\text{diag}}) = S(\rho^{\text{diag}}) - S(\rho), \quad (8)$$

where $S(\rho|\sigma) = \text{tr}(\rho(\log_2 \rho - \log_2 \sigma))$ is the relative entropy [41] and ρ^{diag} is diagonal version of considered density matrix with respect to some fixed orthonormal basis $T = \{|e_k\rangle\}_{k=1}^d$

$$\rho^{\text{diag}} = \sum_{k=1}^d \langle e_k | \rho | e_k \rangle |e_k\rangle \langle e_k|. \quad (9)$$

The choice of the basis T can be described by a unitary transformation that maps the original computational basis to a specific one

$$\hat{T} = \sum_{k=1}^d |e_k\rangle \langle k| : \quad \forall k \quad |e_k\rangle = \hat{T} |k\rangle. \quad (10)$$

The relative entropy of coherence can be averaged over an ensemble in a reference basis T

$$C_T(\mathcal{E}) = \sum_i p_i C_{\text{rel.}}(\hat{T} \rho_i \hat{T}^\dagger), \quad (11)$$

where $\mathcal{E} = \{p_i, \rho_i\}_i$ is a considered ensemble and $\hat{T} \rho_i \hat{T}^\dagger$ is the form of the density matrix ρ_i in the basis T .

Here, we study the basis-free coherence [28] of an ensemble, that is obtained from the latter quantity as a minimum over all orthonormal bases

$$C(\mathcal{E}) = \min_T C_T(\mathcal{E}) = \min_T \sum_i p_i C_{\text{rel.}}(\hat{T} \rho_i \hat{T}^\dagger). \quad (12)$$

Similar definition of the ensemble's basis-free coherence is introduced in Refs. [25–27]. Defined basis-free ensemble coherence shows to what extent density matrices of an ensemble can be simultaneously diagonalized in the same basis. Yet, this quantity requires optimization over all bases in Bob's subspace.

Studied ensemble coherence is, in fact, generalization of the standard relative entropy of coherence for a single state, Eq. (8). One can always reduce ensemble coherence to a trivial state coherence by shrinking an ensemble into a trivial ensemble consisting of a single state. Consider an arbitrary ensemble $\{p_i, \eta_i\}_i$ ($i = 1, \dots, N$) and a fixed basis T . Then, we add an arbitrary density matrix ρ as a perturbation in the examined ensemble. Let δ be the probability of the perturbation density matrix in the modified ensemble \mathcal{E}

$$\mathcal{E} = \{(\delta, \rho), ((1-\delta)p_1, \eta_1), \dots, ((1-\delta)p_N, \eta_N)\}. \quad (13)$$

When the perturbation parameter is zero, $\delta = 0$, we have the original ensemble. With the increase of δ the ensemble loses its initial properties and starts to behave as a single state ρ . As a result, when the perturbation parameter approaches 1, the ensemble coherence in the basis T is equal to the relative entropy of coherence of ρ

$$\lim_{\delta \rightarrow 1} C_T(\mathcal{E}) = C_{\text{rel.}}(\rho). \quad (14)$$

Thus, the definition of ensemble coherence also includes the relative entropy of coherence for a single state and can be considered a general quality of quantumness.

In the previous study [29], the main boundaries on the basis-free coherence were established. Firstly, ensemble's coherence is always upper-bounded by the Holevo quantity [42] of the ensemble

$$C(\mathcal{E}) \leq \chi(\mathcal{E}) = S\left(\sum_{i=1}^N p_i \rho_i\right) - \sum_{i=1}^N p_i S(\rho_i). \quad (15)$$

The right-hand side is closely related to the entanglement consumption. The first term corresponds to the entanglement of the initial Alice-Bob state, while the second term is equal to the average entanglement remaining after the measurement. If the applied measurement is a rank-1 POVM, the ensemble consists only of pure states, and thus, its Holevo quantity is equal to the initial amount of entanglement resource.

In addition, ensemble's coherence is lower-bounded by the gap between the Holevo quantity and accessible information of the ensemble

$$C(\mathcal{E}) \geq \chi(\mathcal{E}) - I_{\text{acc}}(\mathcal{E}) \quad (16)$$

This lower bound was independently presented in Refs. [25–27] and Ref. [29]. The Holevo quantity characterizes the maximum amount of information that can be extracted from an ensemble using collective measurements, whereas the accessible information refers to the maximum information obtainable via individual measurements [43–46]. The presence of quantum properties in an ensemble is indicated by the advantage of collective measurements in terms of extractable information. If all states in the ensemble can be diagonalized in the same basis, the Holevo quantity is achieved by the von Neumann measurement in that basis. In such cases, the information extractable via collective measurements coincides with the accessible information.

III. Pair of non-orthogonal states

As a first example of obtaining coherence from entanglement, we consider the qubit case ($d = 2$) and a von Neumann measurement in the Hadamard basis, $\mathcal{M}_H = \{|+\rangle\langle +|, |-\rangle\langle -|\}$, applied to Alice's subsystem. The Hadamard basis is mutually unbiased with respect to the computational basis, which forms part of the Schmidt basis. Despite the simplicity of the considered POVM, it generates an ensemble with non-zero coherence. Let Alice and Bob share non-ideally entangled bipartite state

$$|\Psi\rangle_{AB} = \cos \alpha |0\rangle_A |0\rangle_B + \sin \alpha |1\rangle_A |1\rangle_B, \quad (17)$$

$$0 \leq \alpha \leq \pi/2,$$

where $\cos \alpha$ and $\sin \alpha$ are the Schmidt coefficients. For $\alpha = \pi/4$ we have the maximally entangled state. Applying the observable \mathcal{M}_H to Alice's subsystem produces the ensemble of two pure states $\mathcal{E}_{B92} = \{p_i, |\psi_i\rangle_B\}_{i=1}^2$ in the

subsystem B. Both measurement results are equiprobable, thus, the states in the ensemble are also equiprobable ($p_1 = p_2 = 1/2$). The states in Bob's subsystem have the following form

$$\begin{aligned} |\psi_1\rangle &= \cos \alpha |0\rangle_B + \sin \alpha |1\rangle_B, \\ |\psi_2\rangle &= \cos \alpha |0\rangle_B - \sin \alpha |1\rangle_B. \end{aligned} \quad (18)$$

The obtained ensemble corresponds to the B92 QKD protocol [31] where two non-orthogonal states are utilized to encode logical bits “0” and “1”. If the initial Alice-Bob state is maximally entangled ($\alpha = \pi/4$), the resulting ensemble is a pair of orthogonal states. For $\alpha = 0$ (zero entanglement), both ensemble's states are similar and coincide with the basis state $|0\rangle_B$. In the mentioned cases, no significant quantum properties are expected, as the states in the ensemble can be simultaneously diagonalized. In a potential QKD scenario, these situations lead to a zero key generation rate. When the states in the ensemble are orthogonal, an eavesdropper can measure all transmitted signals without detection and thereby obtain information about the key. When the states are identical, Bob cannot distinguish between logical bits, which also results in no secret key generation.

For other entanglement values, states of the ensemble are non-orthogonal and, thus, cannot be diagonalized simultaneously. Coherence of an ensemble in a fixed reference basis is the entropy of a probability distribution appearing during the von Neumann measurement of an ensemble in this basis. To calculate the coherence, we fix an arbitrary orthogonal basis $T = \{|e_1\rangle, |e_2\rangle\}$ in the subsystem B

$$C_T(\mathcal{E}_{B92}) = \frac{1}{2} h_2(|\langle e_1|\psi_1\rangle|^2) + \frac{1}{2} h_2(|\langle e_1|\psi_2\rangle|^2), \quad (19)$$

where $|e_1\rangle = \cos \theta_T |0\rangle_B + \sin \theta_T |1\rangle_B$, θ_T is a real value basis parameter and $h_2(x) = -x \log_2 x - (1-x) \log_2 (1-x)$ is the binary entropy. Then, we need to minimize the latter equation over all bases. We have only one real value parameter in the optimization problem.

Figure 1 shows the minimum coherence value of equiprobable non-orthogonal states as a function of the initial entanglement (solid line). In the current work, we consider POVM consisting of only rank-1 elements. Thus, after the applying an observable to the subsystem A, no residual entanglement left. All the initial entanglement is consumed and converted to coherence and accessible information of the ensemble. As expected above, coherence turns to zero, when the initial entanglement is zero or maximal. For the small values of the entanglement (≤ 0.4) the minimum coherence has a linear dependency with the unit slope. As a result, if the initial entanglement is less than 0.4, by applying the Hadamard measurement we obtain ensemble with the coherence equals to the initial entanglement.

$$C(\mathcal{E}_{B92}) = E, \quad \text{if } E \leq 0.4 \quad (20)$$

As highlighted in the previous section, the basis-free coherence of an ensemble is upper-bounded by its Holevo

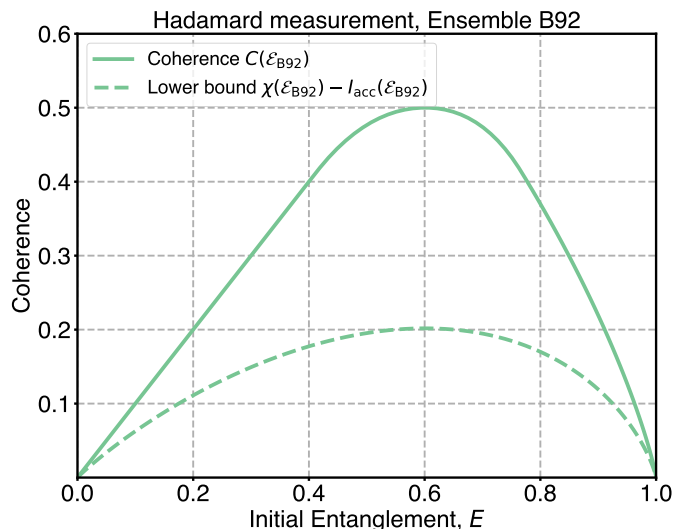


FIG. 1: **Coherence of two non-orthogonal states.** Basis-free coherence and the lower bound on the basis-free coherence as functions of the initial entanglement for a pair of pure non-orthogonal equiprobable states. Solid line stands for the coherence values. Dashed line corresponds to the values of the lower bound

quantity, see Eq. (15). For ensembles of pure states, the Holevo quantity equals the initial entanglement resource. Within the considered range of initial entanglement, the coherence reaches this upper bound. Thus, we identify an optimal strategy within this entanglement range, where coherence attains its maximum achievable value.

The optimal basis for which minimal coherence value equals entanglement is the standard computational basis $T = \{|0\rangle, |1\rangle\}$. In the computational basis, Eq. (19) transforms into entropy of squared Schmidt coefficients, i.e. into the initial entanglement measure. The ensemble is symmetric with respect to the first basis state and tends to align it. Both density matrices are almost diagonal and, thus, the coherence naturally reaches its minimum.

The lower bound on the basis-free coherence is the gap between the Holevo quantity and accessible information of an ensemble and, thus, requires optimization over rank-1 observables. However, for the considered ensemble of two pure states, accessible information can be calculated according to the analytical formula [47] as well as the Holevo quantity

$$\begin{aligned} I_{\text{acc}}(\mathcal{E}_{B92}) &= 1 - h_2\left(\frac{1 + \sqrt{1 - |\langle \psi_1|\psi_2\rangle|^2}}{2}\right), \\ \chi(\mathcal{E}_{B92}) &= h_2\left(\frac{1 - |\langle \psi_1|\psi_2\rangle|}{2}\right). \end{aligned} \quad (21)$$

Figure 1 also represents the coherence lower bound obtained analytically as a function of the initial entanglement (dashed line). The exact values of the lower bound differ from the corresponding coherence values. Mean-

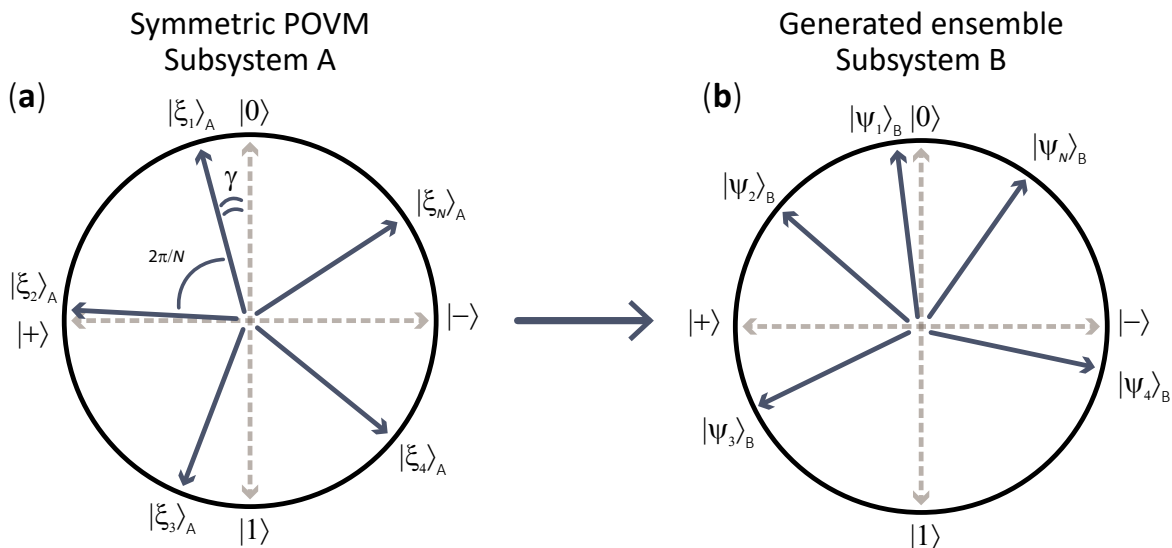


FIG. 2: **Scheme of the ensemble generation.** (a) Structure of the rank-1 POVM built upon the set of symmetric states in Alice’s subsystem. $N = 5$. (b) Generated ensemble in Bob’s subsystem, $N = 5$. When the initial entangled state is the Bell state, the ensemble’s structure coincides with the symmetric states on Alice’s side. When the entanglement decreases to zero, Bob’s ensemble shrinks to the zero basis state $|0\rangle_B$.

while, its behavior with the raise of the initial entanglement corresponds well to coherence. Both quantities reach their maximums when the angle between states of the ensemble is $\pi/4$ or, equivalently, when the initial entanglement E is almost 0.6.

A similar result was obtained in Ref. [16], where the advantage of the Holevo quantity over accessible information was proposed as a measure of quantumness for a pair of non-orthogonal states. Subsequent formal studies on the quantumness of ensembles have also focused on two non-orthogonal states [6, 18, 20, 24–27]. According to most quantumness measures, the ensemble is maximally quantum when the angle between the states is $\pi/4$. Refs. [25, 27] provide plots of quantumness measures for the B92 ensemble that are similar to Fig. 1. In this work, we reinterpret the existing results for the B92 ensemble within a more comprehensive entanglement-based framework for ensemble coherence. In our case, basis-free coherence serves as an upper bound on the gap between the Holevo quantity and accessible information. Nevertheless, we recover the same conclusion: the ensemble of two non-orthogonal states is most quantum when the angle between them is $\pi/4$.

IV. Symmetric observable

Another potential approach to obtain coherence from a given amount of entanglement is to apply an observable with high uncertainty. Intuitively, such an observable must produce a large number of measurement outcomes compared to the dimension of subsystem A. Increasing the number of POVM elements leads to higher entropy

of the measurement results. The resulting ensemble will also consist of a large number of states that cannot be simultaneously diagonalized in the same basis. Namely, we consider a rank-1 observable built upon symmetric pure states [48–52], see Fig. 2a. In this section, we attempt to answer the following question: if the number of POVM elements increases infinitely, what is the limit for ensemble coherence?

As in the previous section, we consider an entangled state of qubit subsystems A and B, Eq. (17). Alice applies a local rank-1 observable which elements are built on the symmetric states

$$\mathcal{M}_{\text{sym}} = \left\{ \frac{2}{N} |\xi_i\rangle\langle\xi_i| \right\}_{i=1}^N, \quad (22)$$

where

$$|\xi_i\rangle = \cos\left(\frac{\theta_i}{2}\right) |0\rangle_A + \sin\left(\frac{\theta_i}{2}\right) |1\rangle_A, \quad (23)$$

$$\theta_i = \gamma + 2\pi(i-1)/N,$$

where free parameter γ is the angle between $|0\rangle_A$ and $|\xi_1\rangle$, $0 \leq \gamma \leq \pi/N$, see Fig. 2a. The states $|\xi_i\rangle$ are symmetric, meaning that each state can be obtained from a previous state by the same unitary transformation \hat{U} : $|\xi_i\rangle = \hat{U} |\xi_{i-1}\rangle$. In this case, the observable is called symmetric with respect to \hat{U} . In our case, \hat{U} has the form

$$\hat{U} = \cos\left(\frac{\pi}{N}\right) \hat{1} - i \sin\left(\frac{\pi}{N}\right) \hat{\sigma}_y, \quad (24)$$

where $\hat{1}$ is the identity operator and $\hat{\sigma}_y$ is Y Pauli matrix. In this section, the unitary transformation is the amplitude rotation around the Y -axis on the Bloch sphere.

For $N = 2$, the considered observable corresponds to a von Neumann measurement; for $N = 3$, it is constructed from the states used in the three-state QKD protocol [33, 34]; and for $N = 4$, it represents a POVM built from states forming two mutually unbiased bases, similar to those in BB84 QKD.

The probability of the i -th measurement result is

$$p_i = \frac{2}{N} \left(\cos^2 \left(\frac{\theta_i}{2} \right) \cos^2 \alpha + \sin^2 \left(\frac{\theta_i}{2} \right) \sin^2 \alpha \right). \quad (25)$$

In the case of the maximally entangled Alice-Bob state, $\alpha = \pi/4$, the resulting probability distribution is uniform.

The exact form of the obtained ensemble $\mathcal{E}_{\text{sym}} = \{p_i, |\psi_i\rangle\}_{i=1}^N$ can be obtained from the operators of the initial POVM and probability distribution of the measurement results

$$|\psi_i\rangle = \sqrt{\frac{2}{Np_i}} \left(\cos \alpha \cos \left(\frac{\theta_i}{2} \right) |0\rangle_{\text{B}} + \sin \alpha \sin \left(\frac{\theta_i}{2} \right) |1\rangle_{\text{B}} \right). \quad (26)$$

The visual structure of the ensemble's states is represented on Fig. 2b. When the initial entangled state is the Bell state, the ensemble's structure fully coincides with the states the observable built upon. In the absence of entanglement, any ensemble fully shrinks into the basis state $|0\rangle_{\text{B}}$.

To calculate the ensemble coherence, we fix an arbitrary orthogonal basis $T = \{|e_1\rangle, |e_2\rangle\}$ in the subsystem B, where $|e_1\rangle = \cos(\theta_T/2) |0\rangle_{\text{B}} + \sin(\theta_T/2) |1\rangle_{\text{B}}$ and θ_T is a real value basis parameter. Coherence in the fixed basis T has the following form

$$C_T(\mathcal{E}_{\text{sym}}) = \sum_{i=1}^N p_i h_2(|\langle e_1 | \psi_i \rangle|^2). \quad (27)$$

To get the coherence minimum over all bases we have to optimize the latter expression over the basis parameter. In our optimization, the basis parameters ranges from 0 to $\pi/2$. Alice is free to choose the parameter γ to maximize the resulting ensemble coherence. The parameter γ ranges from 0 to π/N , as any further increase does not yield different coherence values due to the symmetry of the considered observables.

Figure 3 shows the dependence of the ensemble's informational characteristics on the initial entanglement for different numbers of elements in the applied observable. The solid lines correspond to the basis-free coherence. Meanwhile, dashed lines represent the lower bound on coherence, based on the gap between the Holevo quantity and the accessible information. Colors of the lines reflect the number of elements in the POVM. In this setup, the maximum coherence is around 0.56 for $N = 25$ and is naturally achieved for the ideally entangled state. The

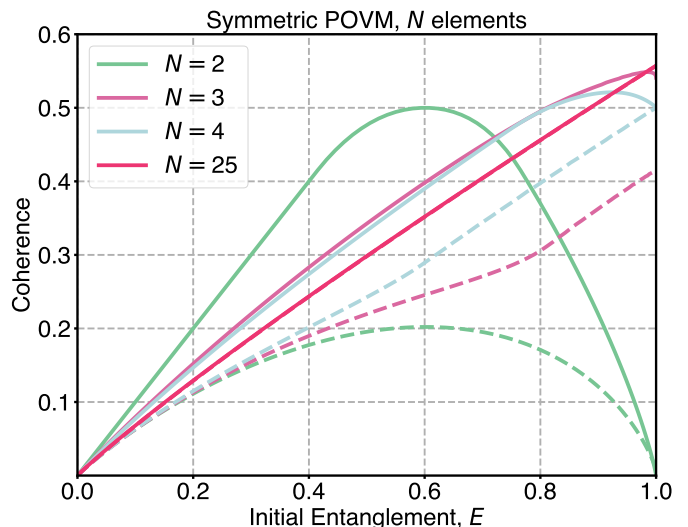


FIG. 3: **Coherence generated with symmetric POVM** Basis-free coherence and the gap between the Holevo quantity and accessible information as functions of the initial entanglement resource, for different numbers of POVM elements $N = 2, 3, 4, 25$. Different colors correspond to different values of N . Solid lines represent coherence values, while dashed lines indicate the corresponding lower bounds. For $N = 25$, the solid and dashed lines coincide.

coherence values rapidly achieve saturation with the increase of N . Further increase of the number of POVM elements does not result in higher coherence.

One may note that there is no dashed line for $N = 25$ on Fig. 3. It coincides with the solid line, standing for coherence. Thus, in the limit of sufficiently large N , the lower bound approaches the coherence and the following equality holds

$$E = \lim_{N \rightarrow \infty} (C(\mathcal{E}_{\text{sym}}) + I_{\text{acc}}(\mathcal{E}_{\text{sym}})). \quad (28)$$

The initial entanglement is fully consumed and splits into the ensemble's coherence and accessible information.

Depending on the amount of entanglement, different observables yield maximal coherence. Within the considered class of POVMs, the two-element observable is optimal for most values of entanglement. In the vicinity of maximal entanglement, the optimal POVM corresponds to a sufficiently large number of elements N . As a result, no single POVM within the class can be identified as universally optimal for coherence generation. In contrast, the behavior of the gap between the Holevo quantity and accessible information exhibits a different trend: this gap increases with increasing N . For example, the observable with three elements consistently yields a higher lower bound values compared to the case of two non-orthogonal states. Similarly, a BB84-like observable outperforms POVM with $N = 3$ in terms of the gap between the Holevo quantity and accessible information, see dashed lines on Fig. 3.

Similar ensembles have been considered as specific examples in several studies [18, 20, 24, 27]. In this work, we reinterpret these ensembles within an entanglement-based framework using a class of symmetric observables. The ensembles studied in the aforementioned works correspond to performing corresponding measurements on one half of a maximally entangled state. For instance, to generate the BB84 ensemble on Bob’s side, one must apply the BB84 POVM on Alice’s subsystem. Our approach reveals how the properties of the resulting ensemble depend on the amount of initial entanglement resource. While Refs. [18, 20, 24] report a strict ordering of quantumness among ensembles, our entanglement-based analysis shows that the optimality of a given ensemble depends on the available entanglement, as discussed above.

V. Conclusion

In this study, for the binary case, we demonstrate how an ensemble with explicit quantum properties can be generated via a von Neumann measurement in the Hadamard basis, which is unbiased with respect to the computational basis forming the Schmidt basis. The resulting ensemble consists of non-orthogonal states corresponding to the B92 QKD protocol, see Sec. III. This ensemble exhibits zero coherence when the initial entanglement is either zero or maximal. This behavior has a clear interpretation in the context of quantum cryptography: When the initial state is maximally entangled, the resulting ensemble consists of orthogonal states which can be perfectly distinguished by an eavesdropper without being detected. Conversely, in the absence of entanglement, the ensemble collapses to identical states, mak-

ing it impossible for the receiver to distinguish logical bits. Both extremes result in a zero secret key generation rate. The considered pair of non-orthogonal states is maximally quantum when their overlap is $1/\sqrt{2}$ — a result consistent with the findings initiated by C.A. Fuchs and developed further in a number of studies. Notably, the basis-free coherence of the ensemble equals the initial entanglement resource for entanglement values up to $E \leq 0.4$. Within a specific range of entanglement, the coherence reaches its upper bound, indicating that the proposed strategy for entanglement-to-coherence conversion is optimal.

As a second example, we consider a class of symmetric observables, see Sec. IV. Each observable in this class is a rank-1 POVM constructed from symmetric states. In the case of maximal entanglement, this class allows the generation of ensembles corresponding to BB84 and three-state QKD protocols. The number of POVM elements can be increased indefinitely, leading to a saturation point. In this regime, the initial entanglement equals the sum of the accessible information and the basis-free coherence of the ensemble. Depending on the given amount of entanglement, different ensembles exhibit varying degrees of coherence. In contrast to the fixed ordering of ensemble quantumness found in previous studies, we observe that the optimality of a particular ensemble depends on the amount of entanglement.

However, within the considered class of observables, we did not identify a universal strategy for obtaining coherence equal to the initial entanglement. Further strategies for constructing such a class of observables will require extending the analysis to the entire Bloch sphere, rather than restricting it to the XZ -plane. This extended class should include, for example, the six-state QKD observable and the SIC-POVM.

-
- [1] M. Jammer, Wiley, New York pp. 121–132 (1974).
 - [2] W. K. Wootters and W. H. Zurek, *Physical Review D* **19**, 473 (1979).
 - [3] B.-G. Englert, *Physical review letters* **77**, 2154 (1996).
 - [4] T. Baumgratz, M. Cramer, and M. B. Plenio, *Physical review letters* **113**, 140401 (2014).
 - [5] S. Luo and Y. Sun, *Physical Review A* **96**, 022130 (2017).
 - [6] X.-F. Qi, T. Gao, and F.-L. Yan, *Frontiers of Physics* **13**, 1 (2018).
 - [7] X. Yuan, G. Bai, T. Peng, and X. Ma, *Physical Review A* **96**, 032313 (2017).
 - [8] A. Streltsov, G. Adesso, and M. B. Plenio, *Reviews of Modern Physics* **89**, 041003 (2017).
 - [9] A. Shlyakhov, V. Zemlyanov, M. Suslov, A. V. Lebedev, G. S. Paraoanu, G. B. Lesovik, and G. Blatter, *Physical Review A* **97**, 022115 (2018).
 - [10] M.-M. Du, H.-W. Li, Z. Tao, S.-T. Shen, X.-J. Yan, X.-Y. Li, W. Zhong, Y.-B. Sheng, and L. Zhou, *The European Physical Journal C* **84**, 838 (2024).
 - [11] M. Piani, S. Gharibian, G. Adesso, J. Calsamiglia, P. Horodecki, and A. Winter, *Physical review letters* **106**, 220403 (2011).
 - [12] A. Streltsov, U. Singh, H. S. Dhar, M. N. Bera, and G. Adesso, *Physical review letters* **115**, 020403 (2015).
 - [13] J. Ma, B. Yadin, D. Girolami, V. Vedral, and M. Gu, *Physical review letters* **116**, 160407 (2016).
 - [14] E. Chitambar and G. Gour, *Reviews of modern physics* **91**, 025001 (2019).
 - [15] M. Takahashi, S. Rana, and A. Streltsov, *Physical Review A* **105**, L060401 (2022).
 - [16] C. A. Fuchs, in *Quantum Communication, Computing, and Measurement 2* (Springer, 2002), pp. 11–16.
 - [17] C. A. Fuchs and M. Sasaki, arXiv preprint [quant-ph/0302108](https://arxiv.org/abs/quant-ph/0302108) (2003).
 - [18] Y. Sun, S. Luo, and X. Lei, *Europhysics Letters* **134**, 30003 (2021).
 - [19] Y. Sun and S. Luo, *Physica Scripta* **96**, 125025 (2021).
 - [20] Y. Fan and M. Zhang, *Physics Letters A* **508**, 129506 (2024).
 - [21] G. Gour, I. Marvian, and R. W. Spekkens, *Physical Review A—Atomic, Molecular, and Optical Physics* **80**, 012307 (2009).

- [22] A. Winter and D. Yang, Physical review letters **116**, 120404 (2016).
- [23] L.-H. Shao, Z. Xi, H. Fan, and Y. Li, Physical Review A **91**, 042120 (2015).
- [24] W. Yuan, Z. Wu, and S.-M. Fei, International Journal of Theoretical Physics **61**, 169 (2022).
- [25] S. Luo, N. Li, and X. Cao, Periodica Mathematica Hungarica **59**, 223 (2009).
- [26] S. Luo, N. Li, and W. Sun, Quantum Information Processing **9**, 711 (2010).
- [27] S. Luo, N. Li, and S. Fu, Theoretical and Mathematical Physics **169**, 1724 (2011).
- [28] D. Kronberg, Lobachevskii Journal of Mathematics **40**, 1507 (2019).
- [29] A. Kodukhov and D. Kronberg, Physical Review A **108**, 052429 (2023).
- [30] L. P. Hughston, R. Jozsa, and W. K. Wootters, Physics Letters A **183**, 14 (1993).
- [31] C. H. Bennett, Physical review letters **68**, 3121 (1992).
- [32] C. H. Bennett and G. Brassard, Theor. Comput. Sci. **560**, 7 (2014), ISSN 0304-3975, theoretical Aspects of Quantum Cryptography – celebrating 30 years of BB84.
- [33] S. J. Phoenix, S. M. Barnett, and A. Chefles, Journal of modern optics **47**, 507 (2000).
- [34] J.-C. Boileau, K. Tamaki, J. Batuwantudawe, R. Laflamme, and J. M. Renes, Physical review letters **94**, 040503 (2005).
- [35] C. H. Bennett, H. J. Bernstein, S. Popescu, and B. Schumacher, Physical Review A **53**, 2046 (1996).
- [36] C. H. Bennett, G. Brassard, S. Popescu, B. Schumacher, J. A. Smolin, and W. K. Wootters, Physical review letters **76**, 722 (1996).
- [37] W. K. Wootters, Physical Review Letters **80**, 2245 (1998).
- [38] M. Krishna and K. Parthasarathy, Sankhyā: The Indian Journal of Statistics, Series A pp. 842–851 (2002).
- [39] P. J. Coles, M. Berta, M. Tomamichel, and S. Wehner, Reviews of Modern Physics **89**, 015002 (2017).
- [40] M. J. Hall, Journal of Physics A: Mathematical and Theoretical **51**, 364001 (2018).
- [41] V. Vedral, Reviews of Modern Physics **74**, 197 (2002).
- [42] A. S. Holevo, Probl. Peredachi Inf. **9**, 3 (1973).
- [43] P. W. Shor, Quantum Communication, Computing, and Measurement 3 pp. 107–114 (2002).
- [44] R. König, R. Renner, A. Bariska, and U. Maurer, Phys. Rev. Lett. **98**, 140502 (2007).
- [45] J. Suzuki, S. M. Assad, and B.-G. Englert, Mathematics of Quantum Computation and Quantum Technology. Chapman Hall (2007).
- [46] V. A. Pastushenko and D. A. Kronberg, Entropy **25**, 956 (2023).
- [47] L. B. Levitin, in *Quantum Communications and Measurement* (Springer, 1995), pp. 439–448.
- [48] G. D. Forney, IEEE Transactions on Information Theory **37**, 1241 (1991).
- [49] A. Chefles and S. M. Barnett, Physics letters A **250**, 223 (1998).
- [50] Y. C. Eldar, A. Megretski, and G. C. Verghese, IEEE Transactions on Information Theory **50**, 1198 (2004).
- [51] J. Bae and L.-C. Kwek, Journal of Physics A: Mathematical and Theoretical **48**, 083001 (2015).
- [52] X. Lü, Physical Review A **107**, 022401 (2023).